CHAPTER 35

Hybrid Frequency-Domain KdV Equation for Random Wave Transformation

Hajime Mase[1], M. ASCE, and James T. Kirby[2], M. ASCE

ABSTRACT: This paper develops a hybrid model for random wave transformation by employing a modified spectral model of the KdV equation and a probabilistic bore-type wave breaking model, and compares the numerical predictions with experimental observations. Main results are as follows: 1) Original frequency-domain KdV equation overestimates energy densities, due to over-shoaling term by Green's law in the equation, even in a region where wave breaking is not seen; 2) Modification of the original KdV equation in order to represent shoaling for linear-dispersive component waves leads to better predictions in the non-breaking region; 3) Damping coefficients in the model equation, either estimated from measured spectral densities or the numerically predicted, are in inverse proportion to the water depth and in proportion to the square of frequency, similar to the viscous damping term of the Burgers equation; 4) The hybrid model developed here can predict transformations of random waves satisfactorily, as indicated by comparison of energy spectra, representative wave heights, periods, and crest heights.

INTRODUCTION

The Boussinesq equations include the effects of weak dispersion and nonlinearity under the condition of $\mu^2 = (k_0 h_0)^2 \ll 1$, $\varepsilon = a_0/h_0 \ll 1$, and $O(\mu^2) = O(\varepsilon)$ where k_0, h_0, a_0 are the characteristic wave number, the water depth, and the wave amplitude (Peregrine, 1967; Madsen and Mei, 1969), and are a useful tool for predicting the transformation of shallow water waves. The Boussinesq type equations with a damping term introduced to simulate a turbulence dissipation can predict the change of monochromatic wave height both in the shoaling and the breaking regions (Karambas and Koutitas, 1992).

An efficient method to solve the Boussinesq equations is to deal with the equations in the frequency domain instead of the time domain. The resulting one-dimensional coupled mode equations considering only shoreward-propagating waves can predict the evolution of nearshore field wind waves (Freilich and Guza, 1984; Elgar and Guza, 1985), and the parabolic coupled mode equations can predict the transformation of periodic long waves over two-dimensional topography (Liu et al., 1985). An angular spectrum model of the Boussinesq equations can predict Mach reflection of cnoidal waves well (Kirby, 1990). The KdV equation is consistent with the Boussinesq equations when considering only shoreward-propagating waves. Although the Boussinesq equations and the KdV equation have only the lowest order of nonlinearity, the frequency-domain equations can estimate shoaled wave heights as well as wave

1 Research Assoc., Department of Civil Engrg., Kyoto University, Kyoto, 606, Japan.
2 Assoc. Prof., Department of Civil Engrg., Univ. of Delaware, Newark, DE 19716, USA.

profiles fairly close to the breaking point (Vengayil and Kirby, 1986). Extension of the Boussinesq equations and the KdV equation to improve their dispersion characteristics was studied by Madsen, Murray and Sørensen (1991) and Khangaonkar and LeMehaute (1991).

This paper develops a hybrid model for random wave transformation by employing a modified frequency-domain KdV equation and a probabilistic bore-type wave breaking model. The original frequency-domain (spectral) KdV equation is modified to reproduce the shoaling and the dispersion relation for linear component waves exactly. In order to include energy dissipation due to wave breaking, a damping term is introduced into the modified spectral KdV equation. A form for the coefficient of the damping term is first deduced by inspection of measured spectral energy densities together with calculated densities by the modified spectral KdV equation, and the coefficient is then formulated by using a probabilistic model of expected energy dissipation rate based on the bore model of Thornton and Guza (1983), taking into account the experimental characteristics.

The model equation developed here can be called a hybrid model, since it employs a spectral method and a probabilistic method (individual wave analysis method). Comparisons between experimental observations and numerical predictions by the hybrid model are carried out against energy spectra, representative wave heights, periods, and crest heights.

MODEL EQUATION

Assuming a vertically two-dimensional case, small water depth variation such as $O(|\nabla_h h|) \le O(\mu^2)$, and considering only shoreward-propagating waves (neglecting reflected waves), we reduce the Boussinesq equations to the KdV equation for variable depth as expressed by

$$\zeta_t + \sqrt{gh}\,\zeta_x + \underbrace{\frac{\sqrt{gh}\,h_x}{4h}\,\zeta + \frac{3\sqrt{gh}}{2h}\,\zeta\zeta_x}_{O(\varepsilon)} + \underbrace{\frac{\sqrt{gh}\,h^2}{6}\,\zeta_{xxx}}_{O(\mu^2)} = 0 \quad , \tag{1}$$

where ζ is the surface displacement, h is the water depth, t is the time, and x is the horizontal coordinate. Substituting the Fourier series representation of surface displacement with complex amplitudes, A_n,

$$\zeta = \sum_{n=1}^{\infty} \frac{1}{2} A_n \, e^{i n \left(\int k_1 \, dx - \omega_1 t \right)} + \text{c. c.} \tag{2}$$

into Eq.(1) yields the lowest-order frequency-domain KdV equation, equivalent to the consistent shoaling model of Freilich and Guza (1984):

$$\frac{dA_n}{dx} + \frac{h_x}{4h} A_n - \frac{1}{6} i n^3 k_1^3 h^2 A_n + \frac{3ink_1}{8h} \left[\sum_{l=1}^{n-1} A_l A_{n-l} + 2 \sum_{l=1}^{N-n} A_l^* A_{n+l} \right] = 0 \; ; \quad n = 1, 2, \ldots\ldots, N \quad , \tag{3}$$

where $dA_n/dx \sim O(\varepsilon)$ is assumed. The procedure followed in deriving the above equation follows that of Freilich and Guza (1984), and Liu et al. (1985). The second

term on the left hand side of Eq.(3) represents shoaling by Green's law; that is, the equation for linear waves

$$\frac{dA_n}{dx} = -\frac{h_x}{4h} A_n \tag{4}$$

is integrated to

$$\frac{A_n(x)}{A_n(0)} = \left\{ \frac{h(x)}{h(0)} \right\}^{-1/4} \tag{5}$$

This can be compared to the component form of fully dispersive linear theory, which gives

$$\frac{dA_n}{dx} = -\frac{(C_{g_n})_x}{2C_{g_n}} A_n \ . \tag{6}$$

The integrated form is then

$$\frac{A_n(x)}{A_n(0)} = \left\{ \frac{C_{g_n}(x)}{C_{g_n}(0)} \right\}^{-1/2} \ , \tag{7}$$

which corresponds to the linear shoaling theory. The third term on the left hand side of Eq.(3) represents the effect of dispersion. For linear component waves in uniform depth, Eq.(3) reduces to

$$\frac{dA_n}{dx} - \frac{1}{6} i n^3 k_1^3 h^2 A_n = 0 \ . \tag{8}$$

The resultant surface displacement is described by

$$\zeta = \frac{1}{2} a_n e^{i\left\{\left(n k_1 + \frac{1}{6} n^3 k_1^3 h^2\right) x - n\omega_1 t\right\}} + \text{c. c.} \ . \tag{9}$$

From Eq.(9) the phase speed is given by

$$C_n = \frac{\omega_1}{k_1} \frac{1}{1 + (nk_1 h)^2/6} \ , \tag{10}$$

where $\omega_1/k_1 = \sqrt{gh}$. Eq.(10) is an approximation in shallow water of the dispersion relation,

$$\frac{C_n}{\sqrt{gh}} = \sqrt{\frac{\tanh k_n h}{k_n h}} \ , \tag{11}$$

where k_n is obtained from $(n\omega_1)^2 = g k_n \tanh k_n h$. When we adopt the equation given by

$$\frac{dA_n}{dx} - ink_1 \left[\sqrt{\frac{k_n h}{\tanh k_n h}} - 1 \right] A_n = 0 \tag{12}$$

instead of Eq.(8), we can provide the exact dispersion relation.

In summary a modified version of spectral KdV equation in order to provide exact shoaling and dispersion relation of each frequency mode is obtained by changing the shoaling and the dispersion terms:

$$\frac{dA_n}{dx} + \frac{(C_{g_n})_x}{2C_{g_n}} A_n - ink_1 \left(\sqrt{\frac{k_n h}{\tanh k_n h}} - 1 \right) A_n + \frac{3ink_1}{8h} \times \left[\sum_{l=1}^{n-1} A_l A_{n-l} + 2 \sum_{l=1}^{N-n} A_l^* A_{n+l} \right] = 0 ; \qquad n = 1, 2, \cdots, N . \tag{13}$$

When energy dissipation is taken into account, a damping term $\alpha_n A_n$ should be added to the left hand side of Eq.(13), where α_n is a damping coefficient to be determined theoretically or experimentally:

$$\frac{dA_n}{dx} + \frac{(C_{g_n})_x}{2C_{g_n}} A_n - ink_1 \left(\sqrt{\frac{k_n h}{\tanh k_n h}} - 1 \right) A_n + \frac{3ink_1}{8h} \times \left[\sum_{l=1}^{n-1} A_l A_{n-l} + 2 \sum_{l=1}^{N-n} A_l^* A_{n+l} \right] + \alpha_n A_n = 0 ; \quad n = 1, 2, \cdots, N . \tag{14}$$

Depending on whether α_n is real, image, or complex, change of energy only, phase only, or both energy and phase, respectively, can be introduced. Here we take α_n to be real.

In shallow water the model equation with damping term is transformed to

$$\left(\sum_{n=1}^{N} |A_n|^2 \right)_x + \frac{h_x}{2h} \left(\sum_{n=1}^{N} |A_n|^2 \right) + 2 \sum_{n=1}^{N} \alpha_n |A_n|^2 = 0 , \tag{15}$$

by adding the two equations of Eq.(14) multiplied by A_n* and the complex conjugate of Eq.(14) multiplied by A_n. By using the relation of

$$E = \frac{1}{2} \rho g \sum_{n=1}^{N} |A_n|^2 , \tag{16}$$

Eq.(15) is rewritten as in a form of an energy flux equation:

$$\left(E \sqrt{gh} \right)_x = - \rho g \sqrt{gh} \left(\sum_{n=1}^{N} \alpha_n |A_n|^2 \right) . \tag{17}$$

It is confirmed from Eq.(17) that the α_n is a kind of energy damping coeffieient.

EXPERIMENT ON RANDOM WAVE TRANSFORMATION

Random waves used here were simulated to have the Pierson-Moskowitz speetrum with f_p = 0.6 Hz and f_p = 1.0 Hz (f_p: the peak frequeney), referred as Case 1 and Case 2, respeetively. Dominated wave breaking type seen in Case 1 was plunging, while in Case 2 spilling breakers were dominated. Figure 1 shows a sketeh of experimental setup. Water surface variation were measured by capaeitanee-type wave gauges (WG.1~WG.12) at water depths of 47 cm, 35 cm, 30 cm, 25 cm, 20 em, 17.5 em, 15 cm, 12.5 cm, 10 cm, 7.5 cm, 5.0 cm and 2.5 cm over a 1/20 plane beaeh. The data were recorded by a digital data reeorder at the sampling interval of 0.025 see for about 30 min duration for Case 1 and 20 min for Case 2.

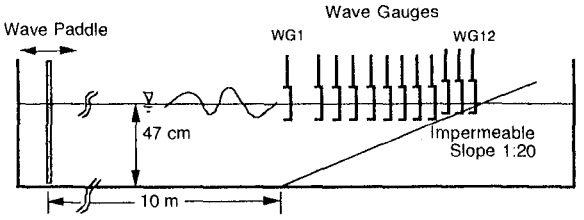

Fig. 1 Experimental Setup.

Figure 2 shows the change of measured energy spectra of Case 1 and Case 2. The data of water surface variations at each wave gauge were split into ten segments of 1024 points with the time interval of 0.1 sec. The energy spectrum of each segment was summed up and averaged. The ensemble averaged spectrum was smoothed by averaging three points. The degree of freedom is 60, and the resolution frequency is 0.03 Hz. The figures show the decay of energies around the initially peak frequency, the shift of peak frequency to the lower frequency, and the increase of energies in lower and higher frequency regions with decrease in the water depth. At the shallowest water of 2.5 cm (WG.12), the energy level of low frequency modes becomes almost the same as that around the initially peak frequency.

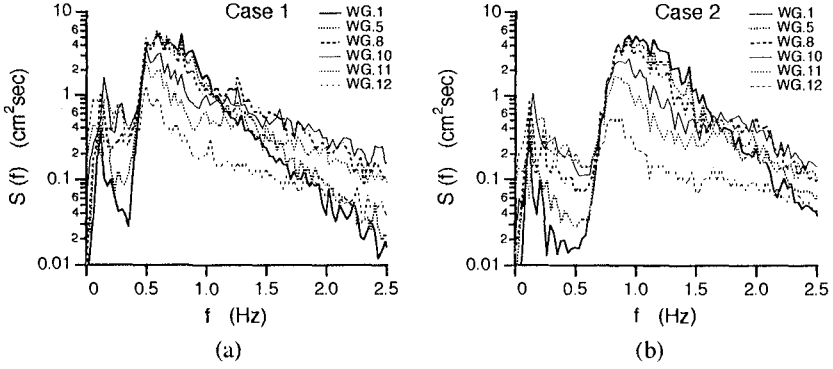

Fig. 2 Change of Measured Energy Spectra.

The calculated spectral energy densities by the original spectral KdV equation (Eq.(4)), the modified spectral KdV model without damping term (Eq.(14)), and the linear shoaling theory were compared with the measured energy densities, as shown in Fig.3. The 300 complex Fourier amplitudes at WG.1 ($h = 47$ cm) were used as input data. The energy spectra were calculated for ten segments and were averaged as in the case of experimental data. The original KdV model overestimates the energy densities at WG.7 where wave breaking is very infrequent. The prediction by the modified KdV model agrees well with the observation at WG.7, but does not at WG.10 where energy dissipation due to wave breaking is important. The result means that since the Green's law is applied to all spectral components by the original KdV model, the overestimation occurs, and that the modified KdV model provides a better prediction outside the surf zone, but results in overestimation in the surf zone, due to the lack of a wave damping

term. The predictions by the linear shoaling theory differ from the observations in spectral shape.

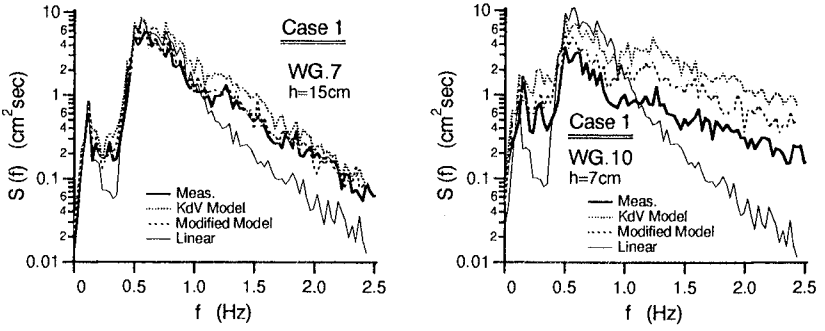

Fig. 3 Comparison between Calculated Results by the Frequency-Domain KdV Model, Modified KdV Model and Linear Shoaling Theory.

DAMPING COEFFICIENT

For constant water depth, the following equation for spectral densities is obtained from Eq.(15) multiplied by $N\Delta t/2$:

$$\sum_{n=1}^{N} \left[(S_n)_x + 2\,\alpha_n S_n \right] = 0 \quad . \tag{18}$$

When α_n is nearly constant for short distance, the solution of Eq.(18) is

$$S_n(\Delta x) = S_n(0)\, e^{-2\alpha_n \Delta x} \quad , \tag{19}$$

and α_n is expressed by

$$\alpha_n = - \ln \left\{ S_n(\Delta x) / S_n(0) \right\} / (2\Delta x) \quad . \tag{20}$$

The Taylor expansion of the above equation is

$$\alpha_n = \left[1 - \left\{ S_n(\Delta x) / S_n(0) \right\} \right] / (2\Delta x) \quad . \tag{21}$$

However, α_n estimated by Eq.(20) or Eq.(21), using the measured spectral energy densities, contains the effects of shoaling and nonlinear wave interaction. Some revision to remove such effects is required. Here the numerical results are utilized. Since the difference between the calculated spectral density at Δx downstream, $S_n(\Delta x)_{Cal.}$, and the measured density at a reference point, $S_n(0)_{Meas.}$, may be considered as the effects of shoaling and nonlinear interaction, the measured spectral density at Δx downstream, $S_n(\Delta x)_{Meas.}$, is modified as

$$S_n'(\Delta x) = S_n(\Delta x)_{Meas.} - \left\{ S_n(\Delta x)_{Cal.} - S_n(0)_{Meas.} \right\} \quad . \tag{22}$$

Since $S_n'(\Delta x)$ takes negative value sometimes and the form of Eq.(20) is inconvenient, Eq.(21) is used as

$$\alpha_n = \left[1 - \left\{ S_n'(\Delta x) / S_n(0)_{\text{Meas.}} \right\} \right] / (2\Delta x) \quad . \tag{23}$$

Another way is to obtain the α_n so as to coincide $S_n(\Delta x)_{\text{Cal.}}$ with $S_n(\Delta x)_{\text{Meas.}}$ described by the following equation:

$$\alpha_n = - \ln \left\{ S_n(\Delta x)_{\text{Meas.}} / S_n(\Delta x)_{\text{Cal.}} \right\} / (2\Delta x) \quad . \tag{24}$$

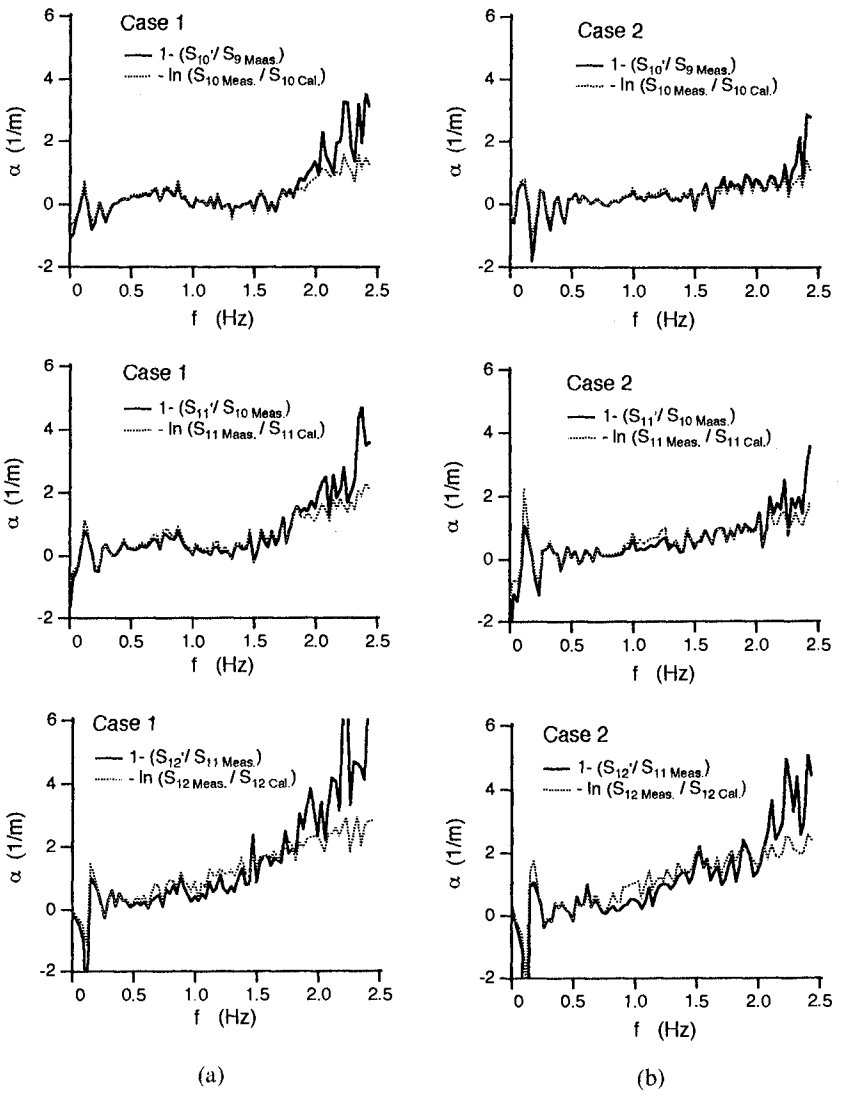

Fig. 4 Estimated Damping Coefficient.

Figure 4 shows the estimated α_n using the data of consecutive wave gauges of WG.9 and WG.10, WG.10 and WG.11, WG.11 and WG.12, separated by 50 cm each other, in which the solid line is the result using Eq.(23) and the dotted line is by Eq.(24). The solid line and the dotted line are almost the same in a region of $f < 2.0$ Hz. The α_n at a given frequency becomes large with decrease in the water depth and appears to be proportional to f^2 with a small constant value. The tendency is similar to that of the viscous damping term of the Burgers equation (given by $-\nu\zeta_{xx}$ where ν is the positive coefficient). The Fourier representation for $-\nu\zeta_{xx}$, using Eq.(2), results in $\nu(nk_1)^2 A_n$, which is rewritten as $\nu(n\omega_1)^2/(gh)\cdot A_n$ using the relation of $(nk_1)^2 = (n\omega_1)^2/(gh)$; that is, $\alpha_n = \omega_n^2/(gh)$. Because of the denominator gh, the α_n becomes large with decrease in the water depth, and is proportional to the frequency squared. These results are used below to guide the choice of the distribution of damping on a frequency-by-frequency basis.

Thornton and Guza (1983) formulated the expected value of energy dissipation rate, $\langle \varepsilon_b \rangle$, based on the probabilistic method (or individual wave analysis method), by using the Rayleigh distribution for wave height distribution, the specific weight function to represent the wave height distribution of broken waves, and an energy dissipation model of bore for each broken wave. The energy flux equation in shallow water is described by

$$\left(E\sqrt{gh}\right)_x = -\langle \varepsilon_b \rangle \ , \tag{25}$$

$$\langle \varepsilon_b \rangle = \frac{3\sqrt{\pi}}{16} \rho g B^3 \bar{f} \frac{H_{\rm rms}^5}{\gamma^2 h^3} \left[1 - \frac{1}{\left\{ 1 + (H_{\rm rms}/\gamma h)^2 \right\}^{5/2}} \right] , \tag{26}$$

where B is a breaking coefficient, $\bar{f}$ is the characteristic frequency, $H_{\rm rms}$ is the r.m.s. wave height, γ is the parameter to relate the $H_{\rm rms}$ with the water depth. Here we choose the parameter values to be

$$B = 1, \ \gamma = 0.6, \ \bar{f} = f_p, \ H_{\rm rms} = 2\sqrt{\sum_n |A_n|^2} \ . \tag{27}$$

The right hand sides of Eqs.(17) and (25) should be equal to each other:

$$\sum_{n=1}^{N} \alpha_n |A_n|^2 = \frac{3\sqrt{\pi}}{16\sqrt{gh}} B^3 \bar{f} \frac{\left(2\sqrt{\sum_n |A_n|^2} \right)^5}{\gamma^2 h^3} \times \left[1 - \frac{1}{\left[1 + \left\{ \left(2\sqrt{\sum_n |A_n|^2} \right) / \gamma h \right\}^2 \right]^{5/2}} \right] \equiv \beta(x) \sum_{n=1}^{N} |A_n|^2 \ . \tag{28}$$

Following Kirby et al. (1992), α_n was determined to represent the experimental tendency as follows:

$$\alpha_n = \alpha_0 + \left(f_n / \bar{f} \right)^2 \alpha_1 \tag{29}$$

$$\alpha_0 = F\cdot\beta, \ \alpha_1 = (\beta - \alpha_0) \frac{\bar{f}^2 \sum_n |A_n|^2}{\sum_n f_n^2 |A_n|^2} \ . \tag{30}$$

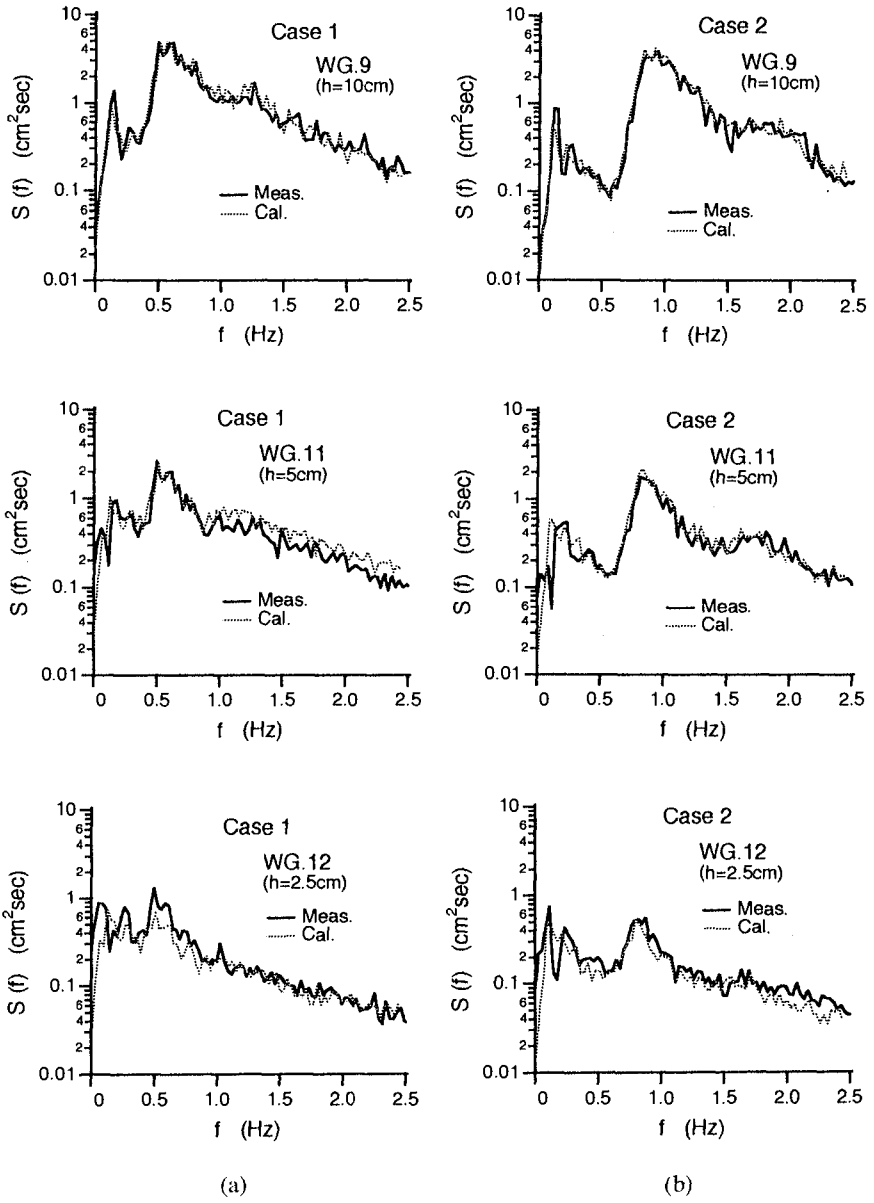

Fig. 5 Comparison between Measured Spectra and Calculated Ones by Hybrid Model Equation.

The first constant term of Eq.(29) represents uniform energy decay over all frequency components, and the second term is to express the f^2 dependence. Here we chose as $F = 0.5$. Eq.(14) using α_n determined by Eqs.(29) and (30) is the hybrid model equation used hereafter. The resulting model is integrated shoreward from the initial gauge position without any subsequent reference to use of measured data.

COMPARISON BETWEEN EXPERIMENTAL OBSERVATIONS AND HYBRID MODEL PREDICTIONS

Figure 5 shows the comparisons of the measured spectra with the calculated ones by the hybrid model equation. Input data was given at WG.1 ($h = 47$ cm). For Case 1, although there are slight differences in the region of $f > 1.0$ Hz at WG.11 and $f < 1.0$ Hz at WG.12, both results agree fairly well. The measured and calculated spectra of Case 2 also show good agreement. Predictions estimate the increase of energies in high and low frequency regions.

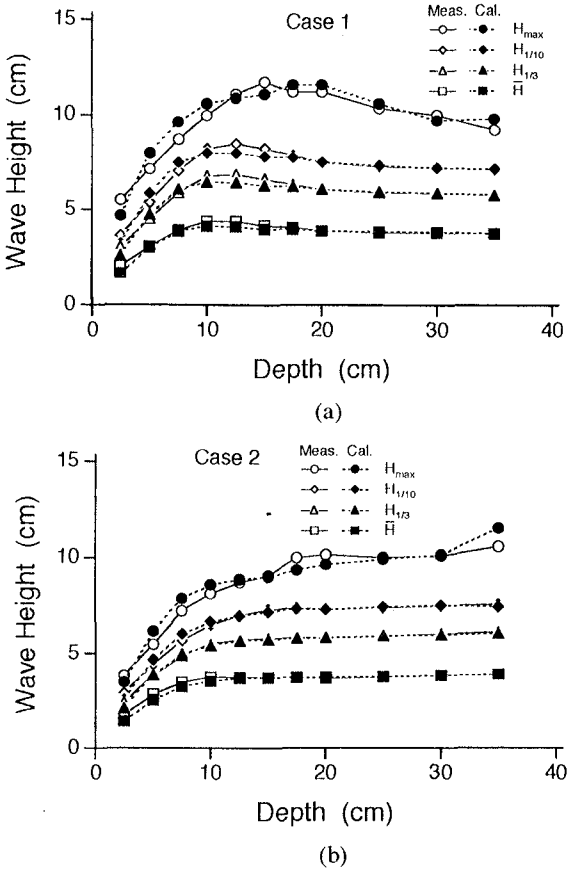

Fig. 6 Comparison between Measured and Calculate Representative Wave Heights.

Using the inverse FFT on the calculated A_n, we can obtain water surface variations from which wave characteristics such as wave heights, periods, crest heights, and so on, can be calculated. In the following comparisons, measured wave characteristics were calculated from the consecutive low-pass filtered (4.0 Hz) water surface variations with Δt =0.025 sec. Figure 6 shows the comparisons of the measured representative wave heights with the calculated ones for Case 1 and Case 2. It can be seen from the figures that the agreement between measured and calculated wave heights is good.

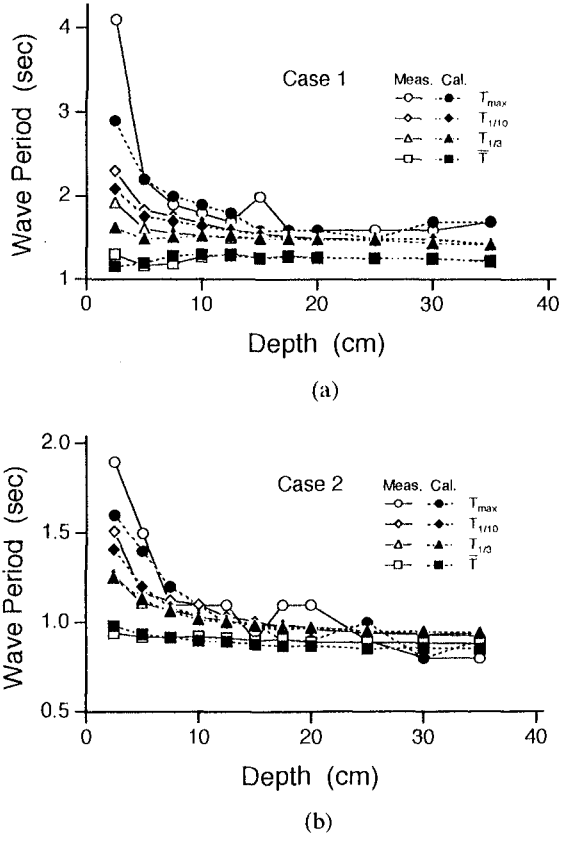

Fig. 7 Comparison between Measured and Calculated Representative Wave Periods.

Figure 7 shows the change of representative wave periods. Existing models based on the individual wave analysis model assume that the wave period is constant, or cannot deal with the change of wave period. Increase of energies of low frequency modes and decrease of energies around the initially peak frequency, according to Fig.2, make the zero-upcrossing periods long compared to the incident wave periods. The present

hybrid model can estimate such change of wave periods, although a little differences can be seen at the shallowest water.

The wave crest height is an important factor for the design of the height of seawalls, platforms, and so on. Figure 8 shows the comparisons between the measured representative crest heights and the calculated ones. Although the predictions are a little smaller than the observations, satisfactorily good agreement is obtained. The representative normalized crest heights (each crest height was normalized by the wave height) are shown in Fig.9, which shows a little different tendency of change between the observations and the predictions. The values themselves agree fairly well.

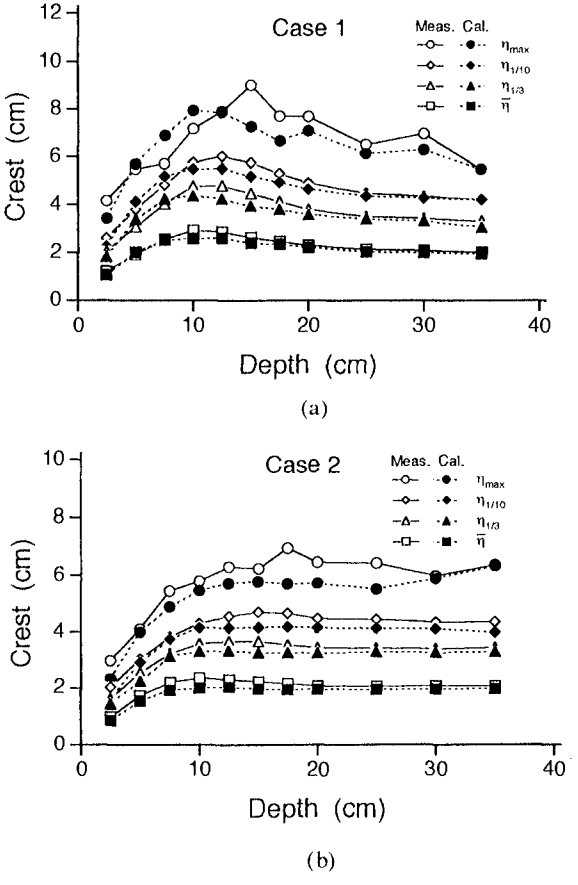

Fig. 8 Comparison between Measured and Calculated Representative Wave Crest Heights.

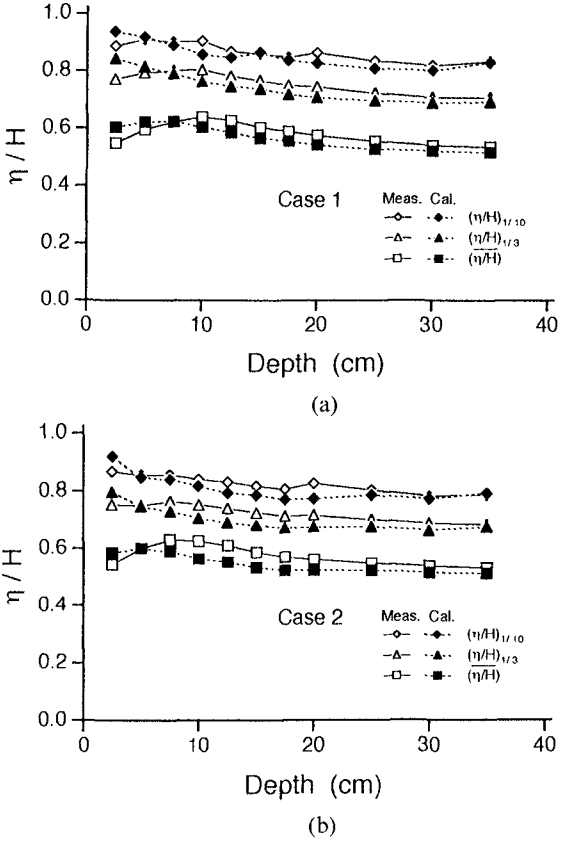

Fig. 9 Representative Normalized Wave Crest Heights.

CONCLUSIONS

This paper proposed a hybrid model for random wave transformation, and compared the numerical predictions with the experimental observations. In the hybrid model a spectral model and a probabilistic model were employed: the former is the modified frequency-domain (spectral) KdV model to provide the shoaling and the dispersion relation for linear component waves with a damping term; the latter is a probabilistic model of energy dissipation due to wave breaking to formulate the coefficient of the damping term in the modified spectral KdV model.

The numerical predictions of energy spectra agreed well the experimental observations concerning the decay of energies around the initially peak frequency, the shift of peak frequency to the lower frequency, and the increase of energies in lower and higher frequency regions with decrease in the water depth. In addition to the energy spectra, the agreement between the predictions and the observation was satisfactorily

good against the representative wave heights, wave periods, wave crest heights. Thus, it was confirmed that the hybrid model developed here was useful as a vertically two-dimensional random waves over a uniform slope. The hybrid model should be further examined on the applicability to other situations such as multiple peak waves over a bar type topography.

REFERENCES

Freilich, M.H. and Guza, R.T. (1984). Nonlinear effects on shoaling surface gravity waves. Phil. Trans. R. Soc. Lond., A311, pp.1-41.

Karambas, Th.V. and Koutitas, C. (1992). A breaking wave propagation model based on the Boussinesq equations. Coastal Engrg., Vol.18, Nos.1 & 2, pp.1-19.

Khangaonkar, T.P. and LeMehaute, B. (1991). Extended KdV equation for transient axisymmetric water waves. Ocean Engrg., Vol.18, No.5, pp.435-450.

Kirby, J.T. (1990). Modelling shoaling directional wave spectra in shallow water. Proc. 22nd Int. Conf. on Coastal Engrg., ASCE, pp.109-122.

Kirby, J.T., Kaihatu, J.M. and Mase, H. (1992). Shoaling and breaking of random wave trains: spectral approaches. Proc. 9th Engrg. Mech. Div. Specialty Conf., ASCE, College Station, pp.71-74.

Liu, P.L.-F., Yoon, S.B. and Kirby, J.T. (1985). Nonlinear refraction-diffraction of waves in shallow water. Jour. Fluid Mech., Vol.153, pp.185-201.

Madsen, O.S. and Mei, C.C. (1969). The transformation of a solitary wave over an uneven bottom. Jour. Fluid Mech., Vol.39, pp.781-791.

Madsen, P.A., Murray, R. and Sørensen, O.R. (1991). A new form of the Boussinesq equations with improved linear dispersion characteristics. Coastal Engrg., Vol.15, No.4, pp.371-388.

Peregrine, D.H. (1967). Long waves on a beach. Jour. Fluid Mech., Vol.27, pp.815-827.

Thornton, E.B. and Guza, R.T. (1983). Transformation of wave height distribution. Jour. Geophys. Res., Vol.88, No.C10, pp.5925-5938.

Vengayil, P. and Kirby, J.T. (1986). Shoaling and reflection of nonlinear shallow water waves. Proc. 20th Int. Conf. on Coastal Eng., ASCE, pp.794-806.